Oil shale pyrolysis products and the fate of sulfur

Birgit Maaten[(a)]*, Oliver Järvik[(a)], Olga Pihl[(b)], Alar Konist[(a)], Andres Siirde[(a)]

[(a)] Department of Energy Technology, Tallinn University of Technology, Ehitajate tee 5, 19086 Tallinn, Estonia
[(b)] Laboratory of Fuels Technology, Virumaa College, Tallinn University of Technology, Järveküla tee 75, 30322 Kohtla-Järve, Estonia

Abstract. *Oil shale (OS) is a solid hydrogen rich fossil fuel whose organic part can, under appropriate conditions, be turned into liquid fuel. The obtained shale oil is a mixture of a large number of organic compounds. However, the exact composition and yield of shale oil depend not only on the composition of oil shale, but also on the type of the reactor where oil was produced, as well as on process parameters like heating rate, pyrolysis temperature, pyrolysis time, and the size of oil shale particles fed to the reactor. In this paper, we present the results of the full chemical analysis of Estonian Ojamaa oil shale – characteristics of oil shale and shale oil and distribution of sulfur. The results of ultimate, proximate, major components and pyrolysis mass balance analyses are also presented and the characteristics of crude shale oil and oil fractions are provided. Special emphasis is put on the analysis of sulfur and its distribution between the pyrolysis products. Additionally, thermogravimetric analysis (TGA) results are provided.*

Keywords: *Ojamaa oil shale, pyrolysis, shale oil fractions, sulfur characteristics.*

1. Introduction

Oil shale (OS) represents a large and mostly untapped hydrocarbon resource. According to the World Energy Council, the world total amount of shale oil reserved in oil shale is about 4.79 trillion barrels, more than that from oil resources which is about 300 billion tons, 4.4 times larger than the current recoverable reserves of crude oil [1, 2]. Estonia is one of the few countries in the world that is utilizing oil shale in significant amounts for both electricity and shale oil production. In 2018, almost 16 Mt of oil shale was mined and of that 8 TWh of electricity and 1.1 Mt of liquid fuels were produced [3]. This satisfies approximately 80% of Estonia's electricity needs, making it one of the least energy dependent countries in the European Union (EU). To

meet the EU criteria for reducing CO_2 emissions also from oil shale industry, older pulverized firing combustion facilities have been equipped with desulfurization and denitrification units. Additionally, circulating fluidized bed (CFB) technology has been implemented which, besides lower emissions, affords also an excellent fuel flexibility without giving in to environmental requirements [4, 5]. However, the use of oil shale in Estonia is directed more and more towards increasing oil production. Due to its properties oil is increasingly used as marine fuel, and new technologies like Enefit-280 have been implemented for this purpose [6]. As shale oil has a complex composition, its full chemical analysis has yet to be performed and results have to be provided.

There are two major deposits of oil shale in Northeast Estonia, Eesti and Tapa. Today both opencast mining and quarry mining are being applied and in 2018, for example, 15.9 Mt of oil shale was mined using these two techniques [3]. Owned by Viru Keemia Grupp, the Ojamaa opencast mine in the Eesti deposit has been actively exploited since 2009 and is the main raw material supplier for shale oil producers today [7]. In this paper, oil shale from the Ojamaa mine was used as a research object. Firstly, Ojamaa was chosen as its optimal location, almost mid-Estonia, was attractive. This kind of oil shale is also found in the Leningrad deposit, which is located in Leningrad Oblast in Northwest Russia, but extends beyond, almost to mid-Estonia. Secondly, the choice was driven by the fact that Ojamaa oil shale had been investigated less than those from other Estonian mines. For example, oil shales from the Aidu quarry and the underground mine Estonia have been thoroughly studied by numerous researchers before [8–13].

Earlier there have been made researches also on Estonian oil shale kerogen. For example, Lille analysed the structure of kerogen and based on that, calculated its different characteristics [14]. At the same time, papers on the full chemical analysis of oil shales by using non-computational methods are scarce.

Therefore, considering the above, this contribution aims to fill in the gap and present the results of the full chemical analysis of Estonian oil shale, on an example of Ojamaa oil shale, as well as characterize its pyrolysis process and the products and residues obtained using non-computational methods such as wavelength-dispersive X-ray fluorescence (WDXRF) spectroscopy and thermogravimetric analysis (TGA). Additionally, pyrolysis tests were run to produce crude oil, then distil it into fractions and characterize their composition.

2. Experimental

2.1. Oil shale

The oil shale sample analysed was from the Ojamaa opencast mine in Northeast Estonia. Prior to analysis, oil shale was dried, crushed and divided for further analysis. The sample was analysed for moisture, ash and mineral CO_2 contents, heating value, component composition, chlorine content, quantifying sulfur in its various forms, etc. The full list of oil shale analyses with the respective standards is given in Table 1. The amounts of carbon, oxygen and sulfur in kerogen, and the contents of inorganic carbon and organic components in oil shale were calculated based on the analysis results obtained.

2.2. Pyrolysis

Additionally, the mass balance for retort pyrolysis is given based on the yields of semicoke, pyrolysis water, gas and shale oil. The production process of oil was carried out in an aluminum retort of 170 ± 10 cm^3 and a condenser of 750 cm^3, in accordance with ISO 647:2017 [15]. Semicoke which was formed in the retort was also analysed. The produced oil was distilled into three fractions that in turn were separately characterized. All the analyses were run according to local and international standards.

2.3. Thermogravimetric analysis

The thermogarvimetric and evolved gas analyses of the oil shale sample were performed using the NETZSCH STA 449 ***F3** Jupiter*® thermal analyser coupled with a NETZSCH QMS *Aëolos*® mass spectrometer (MS). The sample was heated in a high purity nitrogen environment (99.999%) at a heating rate of 20 °C/min in Pt/Rh crucibles with Al_2O_3 liners without lids.

3. Results and discussion

3.1. General characteristics of Ojamaa oil shale

The general characteristics of oil shale from the Ojamaa mine are given in Table 1. For comparison, literature data about other oil shales (OSs) from Estonia as well as selected countries are also presented.

Table 1. General characteristics of Ojamaa oil shale, %wt if not indicated otherwise

Parameter	Standard	Ojamaa OS	Other Estonian OSs [8, 16–18]	Other OSs [19–24]
Ash content (dry basis)	ISO 1171:2010 [25]	51.02	50.5	36.2–75.4
Gross calorific value, dm, MJ/kg	EVS-ISO:1928 [26]	9.85	10.24	4.6–13.4
C^{total}	C, H, N, S, O all EVS-ISO 29541:2015 [27]	27.0	30.5	9.7–32.2
H		2.7	2.7	1.0–4.3
N		0.08	0.2	0.1–0.8
S^{total}		1.72	1.2–1.7	0.3–5.7
O^{total}		17.7	n.a	4.7–28.9
Cl, dm	EVS-EN 196-2:2013 [28]	0.13	n.a	n.a
S_{pyrite}, dm	EVS 664:2017 [29]	1.1	0.96	n.a
$S_{sulfate}$, dm	EVS 664:2017 [29]	0.13	0.07	n.a
Mineral CO_2	ISO 925:2019 [30]	20.9	20.2	1.8–21.0
Total inorganic carbon	n.a	5.7	5.5	n.a
$C_{organic}$	n.a	21.3	25.0	7.9–81
$O_{organic}$	n.a	4.51	n.a	n.a
$S_{organic}$	n.a	0.49	0.43	n.a
Total organic components	n.a	28.97	n.a	n.a

n.a – not available; dm – dry matter; * – US (Green River), Chinese and Pakistan oil shales.

As can be seen from Table 1, Ojamaa oil shale studied in this work was quite similar to another Estonian oil shale, the one from the Estonia mine, as was expected. The nitrogen and total carbon contents were somewhat lower than those found in the literature, whereas the sulfur content was similar to the literature value. The distribution of different forms of sulfur was similar to that established in the literature. The organic carbon content was lower than that of Estonian kukersite from the Estonia mine although their mineral CO_2 contents were the same. Therefore, it can be concluded that the organic carbon content of Ojamaa oil shale was lower than that of other Estonian oil shales reported in the literature.

As oil shale is widely used for power production by combustion, the solid residues need to be analysed in order to prevent problems like slagging, etc. Therefore, laboratory ash was produced at a temperature of 815 °C and characterized according to ISO 540:2008 [31]. The ash fusion parameters are given in Table 2.

Table 2. Ash fusion parameters according to ISO 540:2008 [31]

Parameter, °C	Ojamaa OS	Chinese OS [32]
Deformation temperature	1389	1399
Sphere temperature	1393	Softening 1457
Hemisphere temperature	1395	> 1500
Flow temperature	1408	> 1500

As Table 2 reveals, all ash fusion temperatures are near 1400 °C, with only slight differences between them. It should be noted that the results provided in this paper apply to the cylindrical test object, whereas literature data apply to the research object of pyramid shape. As is known, mineral composition is a key characteristic of ash fusion. For example, an increased content of acidic oxides such as SiO_2, Al_2O_3 and TiO_2, which are all present in oil shale ash, lead to increased ash fusion temperatures, whereas some alkali oxides like CaO, MgO, etc. decrease these temperatures [32].

The Ojamaa oil shale sample and its ash were analysed by XRF for component composition. In addition, the influence of ash composition on ash fusion parameters was investigated. For comparison, the respective data about the ashes of other Estonian and Chinese oil shales are given. The results are presented in Table 3.

Table 3. The composition of Ojamaa oil shale and its ash as determined by XRF, wt%

Component	Ojamaa OS	Ojamaa OS ash	Estonian OSs ash [8, 33, 34]	Chinese OSs ash [24][b]
F	0.15	0.16	n.a	n.a
Na_2O	0.08	0.27	0.13 [8]	0.15–2.4
MgO	3.21	9.78	8.68 [8]	0.21–1.64
Al_2O_3	4.83	15.95	6.08 [8]	4.82–24.82
SiO_2	15.06	21.45	30.74 [8]	46.62–64.08
P_2O_5	0.089	0.30	n.a	2.06–22.9
SO_3	2.75	5.83	n.a	0.07–2.6
Cl	0.19	0.038	0.16–0.54 [33]	n.a
K_2O	1.66	4.08	1.81 [8]	0.55–3.66
CaO	19.79	39.56	39.00 [8]	0.77–25.73
TiO_2	0.225	0.41	n.a	n.a
V	0.003	n.a	n.a	0.038–0.161
Cr	0.004	0.006	n.a	0.033–0.133
Fe_2O_3	1.94	8.00	4.84 [8]	n.a
Ni	0.003	0.004	0.005–0.012 [34]	0.014–0.138
Zn	0.002	0.005	0.013–0.09 [34]	n.a
Br	0.007	n.a	n.a	n.a
Rb	0.003	0.004	n.a	n.a
Sr	0.014	0.024	n.a	0.114–1.558
Zr	0.016	0.028	n.a	0.043–0.215
Ag	0.015	n.a	n.a	n.a
LOI[c]	49.7	48.8	n.a	n.a

n.a – not available; [a] ash of oil shale from the Estonia mine [8] and industrial ash from Balti and Eesti power plants [33, 34]; [b] ash of Chinese Fushun, Huadian, Meihe, Wangqing, Huangxian, Urumqi and Maoming oil shales; [c] LOI – loss on ignition at 920 °C.

As seen from Table 3, the main compounds of Ojamaa oil shale were CaO with 19.79%, SiO_2 with 15.06%, Al_2O_3 with 4.83%, MgO with 3.21%, and minor Fe_2O_3 with 1.94%. The concentrations of other compounds were significantly lower. Na_2O and TiO_2 and elements like Sr and Ag were also present, but with sub-percent concentrations, respectively at 0.08% and 0.22%, and 0.014% and 0.015%. Elements with lower concentrations are not listed in

the table. These results indicate that the characteristic ash fusion temperatures of Ojamaa OS were much lower than those of Chinese OSs, which can be explained by that its SiO_2 content was more than twice lower and CaO about 39% higher, which led to the decrease of the respective temperatures.

For a general description of its thermal decomposition, the sample was subjected to TGA in a 5.0-purity nitrogen environment. The results can be seen in Figure 1.
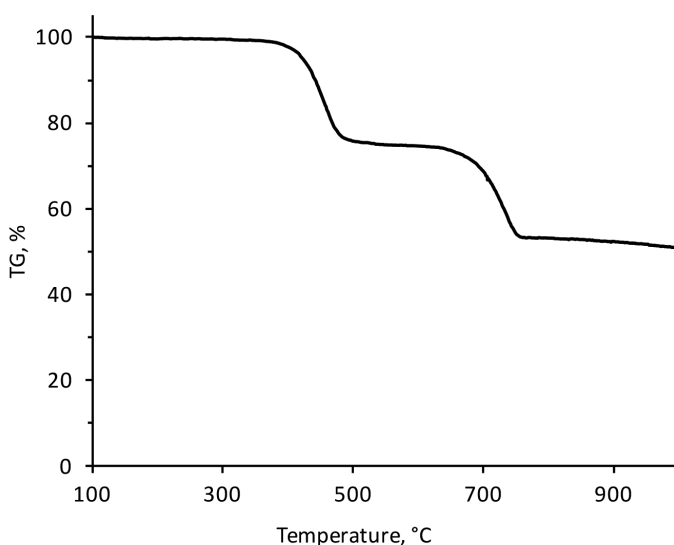

Fig. 1. Thermogravimetric analysis of Ojamaa oil shale.

The figure shows that there were two major mass loss steps during OS thermal decomposition, one in the temperature range of 370–550 °C and the other at 600–780 °C. This was in good agreement with literature findings [10]. The mass loss values were also consistent with those obtained by our group previously, whereas the degree of organic matter decomposition (in the current case, 25%) was a few percent smaller than that reported in the literature. The TGA results for Ojamaa OS were in good agreement with its ash and mineral CO_2 contents presented in Table 1.

3.2. Retort pyrolysis

Pyrolysis tests were run in a standardized Fischer retort according to the international standard ISO 647:2017 [15], to analyse the mass balance and determine the yields of pyrolysis products of Ojamaa oil shale. The data are presented in Table 4. For comparison, the respective literature values for Estonian dictyonema shale and kukersite as well as Chinese Huadian oil shale are given.

Table 4. Pyrolysis product yields of Ojamaa oil shale, wt%

Parameter	Ojamaa OS, Fischer retort	Estonian dictyonema argillite, dry basis [35]	Estonian kukersite, dry basis [35]	Chinese Huadian OS [36]
Oil yield, dry basis, %	16.8	3.62	19.29	15.06
Semicoke, dry basis, %	76.3	89.94	73.81	68.54
Water, dry basis, %	1.7	3.41	1.64	11.14
Gas + losses, dry basis, %	5.2	3.03	5.26	5.26

The oil yields of oil shales around the world vary greatly. Most oil shales have oil yields in the range of 0.5–35%, Australian OS with its 75% yield being an exception [23]. The oil yield value of Ojamaa OS obtained in this study falls in the middle of the above range. Table 4 shows that the pyrolytic water yield and gas and losses data for Ojamaa OS are quite similar to those for kukersite reported in the literature, but there are slight differences in oil and semicoke yields. Compared to dictyonema argillite, Ojamaa oil shale gives about 13% more oil and 13.6% less semicoke. The results obtained in the current work agree with those reported by Järvik et al. [37]. Ojamaa oil shale is considered to be of good quality as 52.1% of its organic components can be converted into oil. Compared to Huadian oil shale, Ojamaa OS affords slightly more oil and semicoke and less water.

The semicoke obtained was analysed for ash, mineral CO_2 contents and elemental composition, the results are presented in Table 5. For comparison, the respective data for semicokes of Estonian and Chinese oil shales are given.

Table 5. The composition of Ojamaa oil shale semicoke, wt%

Parameter	Ojamaa OS semicoke	Other Estonian OS semicoke [38]	Chinese Huadian OS semicoke [39]
Ash	67.1	68.7	77.7
Mineral CO_2	26.0	17.9	n.d
C	14.04	16.3	13.55
H	< 0.1	1.05	0.31
N	< 0.1	n.d	0.22
S^{total}	1.28	1.8	1.12
$S_{sulfate}$	0.12	n.d	n.d
S_{pyrite}	0.08	n.d	n.d
Cl	0.13	n.d	n.d

n.d – not determined

Based on the data given in Table 5, the organic carbon content of Ojamaa OS semicoke was calculated to be 7.1%. For comparison, fresh semicoke of oil shale from the Kiviõli area in Northeast Estonia exhibited an organic carbon content of 7.3% [40]. Table 5 shows the total sulfur content of Ojamaa OS semicoke to be lower than that reported in the literature. This was to be expected because the sulfur content of Kiviõli OS as the starting material was 2.0%, which was 0.3% higher than that of Ojamaa OS. Compared to the finding by Trikkel et al. [38], the partition of sulfur observed in the current work was different as more sulfur was present in the semicoke produced. Ojamaa OS semicoke contained less ash, hydrogen and nitrogen and more carbon and total sulfur than Huadian OS.

The pyrolysis gas evolved during the tests was also analysed for composition. The results are presented in Table 6.

Table 6. Compositional analysis of pyrolysis gas, v/v% if not indicated otherwise

Component	Value
C^{6+}	2.03
Hydrogen	7.91
Methane	12.91
Ethane	8.31
Ethylene	2.38
Propane	3.81
Carbon dioxide	24.69
Propylene	4.05
i-Butane	0.06
n-Butane	1.87
trans-2-Butene	1.69
1-Butene	0.21
2-Methylpropene	0.37
i-Pentane	0.04
n-Pentane	1.12
Hydrogen sulfide	16.33
1,3-Butadiene	n.d
Methylacetylene	0.23
trans-2-Pentene	0.07
2-Methyl-2-butene	1.09
1-Pentene	0.18
Carbonyl sulfide	1.91
Carbon monoxide	8.74
Higher heating value, MJ/kg	37.88
Lower heating value, MJ/kg	34.98

n.d – not determined

According to the table, the major components of pyrolysis gas were carbon dioxide, hydrogen sulfide, methane, ethane and hydrogen. Propane, ethylene, carbonyl sulfide, n-pentane and 2-methyl-2-butene were also found, but with lower concentrations. The concentrations of other components were negligible, below 1 v/v%. Sulfur was mainly present in the form of hydrogen sulfide. These findings comply with the results obtained by other researchers [41–43].

3.3. Shale oil analysis

Although investigators worldwide have applied various experimental techniques to determine the full composition of crude oil of different oil shales, its complex nature has made it quite a challenge. For analysis, sophisticated methods like comprehensive two-dimensional gas chromatography ($GC \times GC$) and multidimensional gas chromatography (MDGC) have been used [44]. In this study, of special interest were the general characteristics and elemental composition of the crude oil of Ojamaa oil shale and the oil fractions obtained. The results are presented in Table 7. For comparison, crude oil data for Chinese Daqing OS are given.

Table 7. General characteristics of crude oil of Ojamaa oil shale

Parameter	Crude oil of Ojamaa OS	Crude oil of Daqing OS [24]
Density at 15 °C, kg/m³	936.4	855.4
Kinematic viscosity, 50 °C, mm²/s	5.48	20.2
Sulfur content, wt%	0.866	0.1
Carbon content, dry basis, wt%	82.28	85.87
Hydrogen content, dry basis,wt%	10.406	13.73
Nitrogen content, dry basis, wt%	0.22	0.16
Flash point in a closed cup, °C	< 0	n.a
Carbon residue, wt%	0.8	2.9
Ash content, wt%	0.011	n.a
Pour point, °C	−31.5	30
Corrosiveness to copper, class	4	n.a
Heat of combustion, MJ/kg	38.634	n.a
Iodine number, gI$_2$/100g	100.6	n.a
Acid number, mg KOH/g	2.3	n.a
Al, mg/kg	< 3	n.a
Si, mg/kg	222	n.a
Na, mg/kg	38	n.a
V, mg/kg	< 1	n.a
Ca, mg/kg	34	n.a
Zn, mg/kg	< 2	n.a
Al, mg/kg	< 3	n.a

n.a – not available

The density of the oil obtained from Ojamaa and Daqing oil shales is usually in the range of 0.8 to 0.98 g/cm^3, the sulfur content varies between 0.4 and 3.5%, and the nitrogen content ranges from 0.1 to 2.1% [23]. Both the sulfur and nitrogen contents of Ojamaa shale oil are in the lower end of the most common values, indicating a promising quality for further applications. The crude shale oil obtained in this work did not contain any significant amounts of metals, silicon with 222 ppm being an exception. Compared to crude oils, metals in Jordanian shale oils exhibit a maximum concentration of 24 ppm, as shown by Abu-Nameh et al. [45]. In comparison with shale oils produced from other oil shales, these amounts can be considered quite low. At the same time, the shale oil from Jordan oil shale contained only 2 ppm vanadium, while the concentrations of nickel and iron were higher, 110 ppm and 145 ppm, respectively [46].

Further the shale oil was distilled into three fractions. Table 8 presents the mass balance of the obtained fractions.

Table 8. Mass balance of oil fractions of Ojamaa oil shale

Fraction	Yield from Ojamaa OS, %
IBP–180 °C	18.5
180–350 °C	44.5
> 350 °C	37.0

IBP – initial boiling point

Cui et al. [47] analysed the composition of heteroatomic compounds in Huadian oil shale by distilling its shale oil into 17 fractions, some of which were of very low cumulative weight. In the current research, Ojamaa shale oil was fractionated into three fractions to offer a more general description of the distillation products obtained. Table 8 reveals that the fractions were not distributed evenly. The 180–350 °C fraction had the highest cumulative weight. As demonstrated by Abu-Nameh et al. [45], a simple distillation of shale oils of different Jordanian oil shales resulted in distilled volumes of about 20% and 90% at temperatures of 180 °C and 350 °C, respectively. As Estonian Ojamaa and Jordanian oil shales are of different geological origin, differences in the results could be expected. In addition, unlike Jordanian shale oils, the fractionation of Ojamaa shale oil was directed more towards the heavier fraction, which resulted in the lower amounts of gasoline and kerosene fractions.

The results of the detailed analysis of the obtained fractions are presented in Table 9.

Table 9. Properties of shale oil fractions obtained from IBP to 350 °C

Parameter	IBP–180 °C	180–350 °C	> 350 °C
Density at 15 °C, kg/m³	769.3	941.1	n.d
Kinematic viscosity, 50 °C, mm²/s	n.d	5.37	n.d
Sulfur content, wt%	0.91	0.749	0.644
Carbon content, dry basis, wt%	84.32	82.32	87.89
Hydrogen content, dry basis, wt%	13.13	10.54	5.90
Nitrogen content, dry basis, wt%	0.12	0.22	0.31
Flash point in a closed cup, °C	< 0	24.0	n.d
Carbon residue, wt	0.1	< 0.1	37.7
Ash content, wt%	n.d	n.d	0.12
Pour point, °C	≤ 42.0	−30.0	n.d
Corrosiveness to copper, class	4	4	n.d
Heat of combustion, MJ/kg	42.04	38.52	36.77
Iodine number, gI$_2$/100g	94.6	89.8	n.d
Acid number, mg KOH/g	n.d	1.7	n.d
Al, mg/kg	n.d	< 3	< 3
Si, mg/kg	n.d	113	345
Na, mg/kg	n.d	96	99
V, mg/kg	n.d	< 1	< 1
Ca, mg/kg	n.d	37	166
Zn, mg/kg	n.d	< 2	< 2

IBP – initial boiling point; n.d – not determined

As Table 9 displays, there are some differences between the three fractions in determined parameter values. For example, the fraction that was distilled in the lowest temperature range contained the most sulfur. Regarding metals, the contents of aluminium, zinc and vanadium were insignificant in the fractions 180–350 °C and > 350 °C. At the same time, the IBP–180 °C fraction did not contain any metals at all. In the 180–350 °C fraction, sodium and silicon were present in quite noticeable amounts, while that of calcium was somewhat lower. Compared to the 180–350 °C fraction, the amounts of Ca and Si in the fraction above 350 °C were higher, while that of Na remained almost the same. Additionally, that same fraction was the only one to exhibit a significant carbon residue – about 38%.

3.4. Characterization of sulfur-containing compounds

In this work, sulfur-containing compounds which greatly determine the quality of the obtained oil were of special interest. The contents of the compounds determined in the low-temperature (IBP–180 °C) fraction are given in Table 10.

Table 10. Sulfur-containing compounds in the IBP–180 °C fraction as determined by GC, mg S/kg if not indicated otherwise

Component	IBP–180 °C[a]
S^{total}, wt%[b]	0.91
Hydrogen sulfide	337.83
Methylmercaptane	45.6
Ethylmercaptane	167.75
Unidentified	n.d
Carbon disulfide	18.69
2-Propanethiol	42.0
Unidentified	n.d
1-Propanethiol	165.11
1-methyl-1-propanethiol	191.3
Thiophene	208.76
2-Methyl-1-propanethiol	8.97
1-Butanethiol	87.29
Unidentified	43.61
2-Methylthiophene	1523.56
3-Methylthiophene	112.62
Unidentified	93.4
1-Pentanethiol	58.31
Unidentified	2169.32
3-Ethylthiophene	477.83
Unidentified	3150.19
Benzothiophene	39.09
Unidentified	163.65
Total identified	3484.7
Total unidentified	5620.2
Total, mgS/kg	9104.9
Total, wt%, gas chromatographically	0.91

IBP – initial boiling point; n.d – not detremined; [a] analysis conditions: heating rate 5 °C/min, maximum temperature 280 °C, 100 m non-polar PetrocolTmDH column, FPD detector, carrier gas helium; [b] EVS-EN ISO 20846:2011 [48].

The different compounds in shale oils have aroused researchers' interest worldwide for a long time already. For example, Willey et al. [49] investigated sulfur heterocycles in coal liquids and shale oils, separating chromatographically and identifying 32 such compounds. However, no quantification of the compounds was performed by the investigators. Recently, a similar research was conducted on kerogen by using an advanced chemical analysis technique, ^{13}C solid-state nuclear magnetic resonance (^{13}C NMR) spectroscopy, to analyse heteroatomic compounds in it [50]. Additionally, Cui et al. [47] investigated heteroatomic compounds in Huadian shale oil and showed C2-benzothiophenes, C3-thiophenes and C2-thiophenes to be the most abundant. As seen from Table 10, only about a third of the compounds were identified and two thirds were not. 2-Methylthiophene, 3-ethylthiophene and hydrogen sulphide had the highest concentrations, while other compounds exhibited lower concentrations. The above results compare quite well with those obtained by Cui et al. [47].

3.5. The distribution of total sulfur

In view of the regulations set for oil production, sulfur distribution is an issue to be handled with utmost care. Namely, the regulations of the International Maritime Organization (IMO) foresee the reduction of the maximum sulfur content in marine fuel oil down to 0.5% globally by 1 January 2020 [51]. These regulations have already led to the reduction of sulfur content of ship emissions.

Different analytical techniques enable the content of sulfur in pyrolysis products to be determined and the distribution of total sulfur analysed. In the present work, the sulfur content in pyrolytic water was found by estimating that the total sulfur content in the water was 1.5 g/L. The contents of the different forms of sulfur in pyrolytic water were not separately determined. As a result, the sulfur content in pyrolysis gas was found as that of residual sulfur. The partition of total and organic sulfur in pyrolysis products is illustrated in Figure 2.

Due to its marginality, the content of pyrolytic water is not well visualized in the figure. It should be kept in mind that the amounts of pyritic and sulfate sulfur in gas were found as a difference. On the basis of the results presented in Tables 1, 3 and 4, it was not possible to define the distribution of pyritic and sulfate sulfur between the oil shale pyrolysis products. However, the authors' experience tells that pyrolytic and sulfate sulfur either remain in semicoke or end up in pyrolytic gas (as non-H$_2$S) or in pyrolytic water and are not transferred into shale oil as organic sulfur. The findings of Elenurm et al. [35], who investigated the partitioning of sulfur during the thermal processing of oil shale, are in support of the above observation. So, when the temperature of semicoking in the reactor is increased from 450 to 480 °C, more sulfur will remain in the ash residue, which results in an increase of the total oil shale
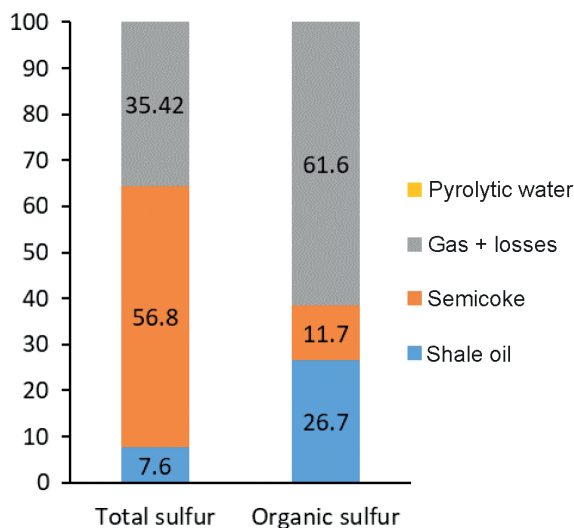
Fig. 2. Distribution of sulfur (mass%) in oil shale pyrolysis products. The pyrolytic water content was estimated to be 1.5 g/L.

sulfur from 61 to 87%. This is mostly due to sulfide sulfur whose content in oil shale increases from 20 to 77%. The amount of organic sulfur decreases only from 1.2 to 1.1% when increasing the retorting temperature. This complies with the results obtained earlier by Pan et al. [52]. Moreover, the researchers found the remainder of the sulfur after pyrolysis to be in the form of hydrogen sulfide.

4. Conclusions

In this study, Estonian oil shale from the Ojamaa mine was subjected to full chemical analysis. The pyrolysis of oil shale was carried out in a standardized Fischer retort. The main pyrolysis products obtained (shale oil, semicoke, gas) were characterized and the results compared with those for other oil shales from around the world. Shale oil was distilled into three fractions which were in turn analysed. Based on the data obtained it was concluded that about 52% of organic matter was converted to shale oil, indicating that oil shale was of good quality. After determining the total sulfur content of the starting material and the products obtained, the distribution of sulfur was analysed. It was concluded that about 50% of sulfur remained in semicoke, about 35% in pyrolysis gas (with some losses) and about 8% in shale oil. Interestingly, most of the organic sulfur was found in pyrolysis gas, whereas shale oil contained approximately 27% organic sulfur and about 12% semicoke.

Acknowledgements

REFERENCES

1. Pan, Y., Zhang, X., Liu, S., Yang, S., Ren, N. A review on technologies for oil shale surface retort. *J. Chem. Soc. Pakistan*, 2012, **34(**6), 1331–1338.
2. World Energy Council. *World Energy Resources: 2013 Survey*. Available: http://www.worldenergy.org/publications/entry/world-energy-resources-2013-survey.
3. *Estonian Oil Shale Industry Yearbook,* 2018. Available: https://www.energia.ee/-/doc/8457332/ettevottest/investorile/pdf/Polevkivi_aastaraamat_2019_eng.pdf
4. Konist, A., Pikkor, H., Neshumayev, D., Loo, L., Järvik, O., Siirde, A., Pihu, T. Co-combustion of coal and oil shale blends in circulating fluidized bed boilers. *Oil Shale*, 2019, **36(**2S), 114–127.
5. Pihu, T., Konist, A., Neshumayev, D., Loo, L., Molodtsov, A., Valtsev, A. Full-scale tests on the co-firing of peat and oil shale in an oil shale fired circulating fluidized bed boiler. *Oil Shale*, 2017, **34**(3), 250–262.
6. Neshumayev, D., Pihu, T., Siirde, A., Järvik, O., Konist, A. Solid heat carrier oil shale retorting technology with integrated CFB technology. *Oil Shale*, 2019, **36**(2S), 99–113.
7. *VKG Mines – Products and Services*. Available: https://www.vkg.ee/keskkond
8. Loo, L., Maaten, B., Siirde, A., Pihu, T., Konist, A. Experimental analysis of the combustion characteristics of Estonian oil shale in air and oxy-fuel atmospheres. *Fuel Process. Technol.*, 2015, **134**, 317–324.
9. Konist, A., Valtsev, A., Loo, L., Pihu, T., Liira, M., Kirsimäe, K. Influence of oxy-fuel combustion of Ca-rich oil shale fuel on carbonate stability and ash composition. *Fuel*, 2015, **139**, 671–677.
10. Maaten, B., Loo, L., Konist, A., Nešumajev, D., Pihu, T., Külaots, I. Decomposition kinetics of American, Chinese and Estonian oil shales kerogen. *Oil Shale*, 2016, **33**(2), 167–183.
11. Külaots, I., Goldfarb, J. L., Suuberg, E. M. Characterization of Chinese, American and Estonian oil shale semicokes and their sorptive potential. *Fuel*, 2010, **89**(11), 3300–3306.
12. Kaljuvee, T., Kuusik, R., Trikkel, A. SO_2 binding into the solid phase during thermooxidation of blends. Estonian oil shale semicoke. *J. Therm. Anal. Calorim.*, 2003, **72**(1), 393–404.
13. Konist, A., Pihu, T., Neshumayev, D., Külaots, I. Low grade fuel – oil shale and biomass co-combustion in CFB boiler. *Oil Shale*, 2013, **30**(2S), 294–304.
14. Lille, Ü. Current knowledge on the origin and structure of Estonian kukersite kerogen. *Oil Shale*, 2003, **20**(3), 253–263.

15. ISO 647:2017. *Brown coals and lignites – Determination of the yields of tar, water, gas and coke residue by low temperature distillation.*

16. Gerasimov, G., Khaskhachikh, V., Potapov, O. Experimental study of kukersite oil shale pyrolysis by solid heat carrier. *Fuel Process. Technol.*, 2017, **158**, 123–129.

17. Maaten, B., Loo, L., Konist, A., Pihu, T., Siirde, A. Investigation of the evolution of sulphur during the thermal degradation of different oil shales. *J. Anal. Appl. Pyrol.*, 2017, **128**, 405–411.

18. Kaljuvee, T., Keelmann, M., Trikkel, A., Kuusik, R. Thermooxidative decomposition of oil shales. *J. Therm. Anal. Calorim.*, 2011, **105**(2), 395–403.

19. Hillier, J. L., Fletcher, T. H., Solum, M. S., Pugmire, R. Characterization of macromolecular structure of pyrolysis products from a Colorado Green River oil shale. *Ind. Eng. Chem. Res.*, 2013, **52**(44), 15522–15532.

20. Tiwari, P., Deo, M., Lin, C. L., Miller, J. D. Characterization of oil shale pore structure before and after pyrolysis by using X-ray micro CT. *Fuel*, 2013, **107**, 547–554.

21. Bai, F., Sun, Y., Liu, Y., Li, Q., Guo, M. Thermal and kinetic characteristics of pyrolysis and combustion of three oil shales. *Energ. Convers. Manage.*, 2015, **97**, 374–381.

22. Williams, P. T., Ahmad, N. Investigation of oil-shale pyrolysis processing conditions using thermogravimetric analysis. *Appl. Energ.*, 2000, **66**(2), 113–133.

23. Altun, N. E., Hicyilmaz, C., Hwang, J.-Y., Bacgi, A. S., Kök, M. V. Oil shales in the world and Turkey; reserves, current situation and future prospects: A review. *Oil Shale*, 2006, **23**(3), 211–227.

24. *Oil Shale – Petroleum Alternative* (Qian, J., Yin, L., Eds. in Chief). China Petrochemical Press, Beijing, 2010.

25. ISO 1171:2010. *Solid mineral fuels – Determination of ash.*

26. EVS-ISO 1928:2016. *Solid mineral fuels. – Determination of gross calorific value by bomb calorimetric method and calculation of net calorific value.*

27. EVS-ISO 29541:2015. *Solid mineral fuels – Determination of total carbon, hydrogen and nitrogen content – Instrumental method.*

28. EVS-EN 196-2:2013. *Method of testing cement – Part 2: Chemical analysis of cement.*

29. EVS 664:2017. *Solid fuels: sulphur content. – Determination of total sulphur and its bonding forms.*

30. ISO 925:2019. *Solid mineral fuels – Determination of carbonate carbon content – Gravimetric method.*

31. ISO 540:2008. *Hard coal and coke – Determination of ash fusibility.*

32. Lu, Y., Wang, Y., Xu, Y., Li, Y., Hao, W., Zhang, Y. Investigation of ash fusion characteristics and migration of sodium during co-combustion of Zhundong coal and oil shale. *Appl. Therm. Eng.*, 2017, **121**, 224–233.

33. Konist, A., Pihu, T., Neshumayev, D., Siirde, A. Oil shale pulverized firing: boiler efficiency, ash balance and flue gas composition. *Oil Shale*, 2013, **30**(1), 6–18.

34. Liiv, S., Kaasik, M. Trace metals in mosses in the Estonian oil shale processing region. *J. Atmos. Chem.*, 2004, **49**(1–3), 563–578.

35. Elenurm, A., Oja, V., Tali, E., Tearo, E., Yanchilin, A. Thermal processing of dictyonema argillite and kukersite oil shale: Transformation and distribution of sulfur compounds in pilot-scale galoter process. *Oil Shale*, 2008, **25**(3), 328–334.

36. Jiang, X. M., Han, X. X., Cui, Z. G. New technology for the comprehensive utilization of Chinese oil shale resources. *Energy*, 2007, **32**(5), 772–777.

37. Järvik, O., Oja, V. Molecular weight distributions and average molecular weights of pyrolysis oils from oil shales: Literature data and measurements by size exclusion chromatography (SEC) and atmospheric solids analysis probe mass spectroscopy (ASAP MS) for oils from four different deposits. *Energ. Fuel.*, 2017, **31**(1), 328–339.

38. Trikkel, A., Kuusik, R., Martins, A., Pihu, T., Stencel, J. M. Utilization of Estonian oil shale semicoke. *Fuel Process. Technol.*, 2008, **89**(8), 756–763.

39. Huang, Y., Zhang, M., Lyu, J., Yang, H. Modeling study of combustion process of oil shale semicoke in a circulating fluidized bed boiler. *Carbon Resour. Convers.*, 2018, **1**(3), 273–278.

40. Saether, O., Banks, D., Kirso, U., Bityukova, L., Sorlie, J. E. The chemistry and mineralogy of waste from retorting and combustion of oil shale. *Geol. Soc. London, Spec. Publ.*, 2004, **236**(1), 263–284.

41. Garcia-Labiano, F., Hampartsoumian, E., Williams, A. Determination of sulfur release and its kinetics in rapid pyrolysis of coal. *Fuel*, 1995, **74**(7), 1072–1079.

42. Garcia, R., Moinelo, S. R., Lafferty, C. J., Snape, C. E. Pyrolytic desulfurization of some high-sulfur coals. *Energ. Fuel.*, 1991, **5**(4), 582–586.

43. Guo, Z., Fu, Z., Wang, S. Sulfur distribution in coke and sulfur removal during pyrolysis. *Fuel Process. Technol.*, 2007, **88**(10), 935–941.

44. Ristic, N. D., Djokic, M. R., Konist, A., Van Geem, K. M., Marin, G. B. Quantitative compositional analysis of Estonian shale oil using comprehensive two dimensional gas chromatography. *Fuel Process. Technol.*, 2017, **167**, 241–249.

45. Abu-Nameh, E. S. M, Al-Ayed, O. S., Jadallah, A. Determination of selected elements in shale oil liquid. *Oil Shale*, 2019, **36**(2S), 179–187.

46. Akash, B. A., Jaber, J. O. Characterization of shale oil as compared to crude oil and some refined petroleum products. *Energ. Source.*, 2003, **25**(12), 1171–1182.

47. Cui, D., Wang, Q., Wang, Z. C., Liu, Q., Pan, S., Bai, J., Liu, B. Compositional analysis of heteroatom compounds in Huadian shale oil using various analytical techniques. *Energ. Fuel.*, 2019, **33**(2), 946–956.

48. EVS-EN ISO 20846:2011. *Petroleum products – Determination of sulfur content of automotive fuels – Ultraviolet fluorescence method*.

49. Willey, C., Iwao, M., Castle, R. N., Lee, M. L. Determination of sulfur heterocycles in coal liquids and shale oils. *Anal. Chem.*, 1981, **53**(3), 400–407.

50. Chu, W., Cao, X., Schmidt-Rohr, K., Birdwell, J. E., Mao, J. Investigation into the effect of heteroatom content on kerogen structure using advanced ^{13}C solid-state nuclear magnetic resonance spectroscopy. *Energ. Fuel.*, 2019, **33**(2), 645–653.

51. Chu Van, T., Ramirez, J., Rainey, T., Ristovski, Z., Brown, R. J. Global impacts of recent IMO regulations on marine fuel oil refining processes and ship emissions. *Transp. Res. D.*, 2019, **70**, 123–134.
52. Pan, S., Wang, Q., Bai, J., Liu, H., Chi, M., Cui, D., Xu, F. Investigation of behavior of sulfur in oil fractions during oil shale pyrolysis. *Energ. Fuel.*, 2019.